Virchows Arch (1999) 434:267–276

CASE REPORT

Akihiro Hemmi · Akira Komiyama · Shinichi Ohno
Yasuhisa Fujii · Nobuo Terada · Ryohei Katoh
Akira Yokoyama · Akira Kawaoi

Autonomic nerve tumour with skeinoid fibres: ultrastructure of skeinoid fibres examined by quick-freezing and deep-etching method

Received: 9 June 1998 / Accepted: 2 September 1998

Abstract A case of gastrointestinal autonomic nerve tumour with skeinoid fibres (SFs) of the jejunum in a 79-year-old Japanese man, was examined by the quick-freezing and deep-etching (QF-DE) method. The tumour consisted of spindle cells with immunohistochemical reactions for vimentin, NSE and CD34. Electron microscopically, features of the neural cells of the myenteric plexus were observed. The QF-DE method demonstrated intercellular meshwork structures, consisting of thin filaments (7–15 nm), with granular deposits. Fully developed parts of the deposits formed nodular aggregates composed of irregularly surfaced thick fibrils (30–48 nm) with a tendency to linear arrangement (SFs). We detected many interconnecting thin filaments (ICTFs) between the SFs, which were pre-existing components in the meshwork, avoiding the granular deposits. The focal thickening formed by the connection between SFs and ICTFs revealed a periodicity typical of SFs (33–45 nm). We conclude that SFs are formed by decoration of the granular deposits along pre-existing intercellular meshwork structures.

Key words Autonomic nerve tumour · Small intestine · Immunohistochemistry · Quick-freezing · Deep-etching

A. Hemmi (✉)[1] · A. Komiyama · R. Katoh · A. Yokoyama
A. Kawaoi
Department of Pathology and Anatomy,
Yamanashi Medical University, 1110 Shimokato, Tamaho,
Yamanashi 409–3898, Japan

S. Ohno · Y. Fujii · N. Terada
Departnment of Anatomy, Yamanashi Medical University,
1110 Shimokato, Tamaho, Yamanashi 409-3898, Japan

Mailing address:
[1] Second Department of Pathology,
Yamanashi Medical University, 1110 Shimokato, Tamaho-cho,
Nakakoma-gun, Yamanashi 409–3898, Japan
e-mail: ahemmi@res.yamanashi-med.ac.jp
Fax: +81-552-73-7108

Introduction

In 1991, Min [27] became the first to report the ultrastructural characteristics of stromal fibrillary aggregates, which were composed of fluffy 45-nm-thick fibrils with periodicity of 41–48 nm, as a useful histological marker for neurogenic spindle cell tumours. He also designated them skeinoid fibres (SFs), because of their resemblance to skeins of yarn. Their histogenesis is still unclear.

We have examined the ultrastructures of SFs in a case of gastrointestinal autonomic nerve tumour (GANT) [14, 15, 22, 43], a newly categorized neurogenic tumour entity among gastrointestinal stromal tumours (GISTs) [32, 37, 41, 42], using the quick-freezing and deep-etching (QF-DE) method. We have already shown that the ultrastructural features of cytoskeleton and extracellular matrices could be clearly observed, even in human surgical specimens, by this method [12, 13], which allows us to examine the three-dimensional ultrastructure of SFs at high resolution. Our purpose in the present study was to clarify the ultrastructural features of the SFs and to discuss their possible histogenesis.

Clinical history

A 79-year-old Japanese man was admitted to Nirasaki Sougo Hospital with melaena on 8 November 1995. In spite of detailed examination by abdominal computed tomography, ultrasound diagnosis, and both gastric and colonic endoscopies, no bleeding site was detected. Symptomatic treatment with blood transfusion (5–6 U/day) was performed, but the patient's physical condition bacame gradually worse. On 15 November 1995 he was transferred to the Second Department of Surgery, Yamanashi Medical University Hospital for further evaluation. His physical checks on admission revealed a large tumour of soft consistency in the abdomen, but no tenderness or acites was recognized.

Laboratory data disclosed low levels of total serum protein (3.3 g/dl), serum albumin (2.2 g/dl), haemoglobin (6.7 g/dl), and haematocrit (18.7%). The CT scanner image, combined with superior mesenteric arteriogram, revealed a vascular abdominal tumour (9×6×8.5 cm in size) fed from a second jejunal artery and confirmed the intestinal bleeding site. A 13-cm-long segment of the jejunum with the tumour was resected on 16 November 1995.

Postoperatively, additional chemotherapy was performed. The patient was discharged from the hospital on 7 December 1995 and subsequently underwent two further operations for abdominal recurrence: excision of a retroperitoneal tumouur on 14 June 1996, and abdomio-perineal excision of the rectum on 26 July 1996. Following the last operation, he suffered an intra-abdominal haemorrhage and peritonitis, and died on 27 August 1996. The chest and abdominal autopsy findings showed severe peritonitis with haemorrhage, but no residual tumour was detected.

His past medical and family histories were noncontributory.

Table 1 Primary antibodies used in this study (*MoAb* monoclonal antibody, *PoAb* polyclonal antibody, + mildly positive, ++ intensely positive, – negative)

Antibodies	Source	Clonality	Dilution	Reactivity
HHF35	DAKO, Denmark	MoAb	1:50	–
Desmin	DAKO	PoAb	1:50	–
αSMA	DAKO	MoAb	1:40	–
Vimentin	DAKO	MoAb	1:50	++
Neuron-specific enolase	DAKO	PoAb	1:50	+
CD34	Immunotech, France	MoAb	1:50	+
S-100 protein	DAKO	PoAb	1:50	–
Synaptophysin	DAKO	PoAb	1:100	–
Chromogranin	DAKO	MoAb	1:100	–
Neurofilament	DAKO	MoAb	1:100	–
HAM-56	DAKO	MoAb	1:50	–
Alpha-1-antitrypsin	DAKO	PoAb	1:50	–
Type IV collagen	LSL, Japan	PoAb	1:1000	–
Laminin	DAKO	PoAb	1:100	–

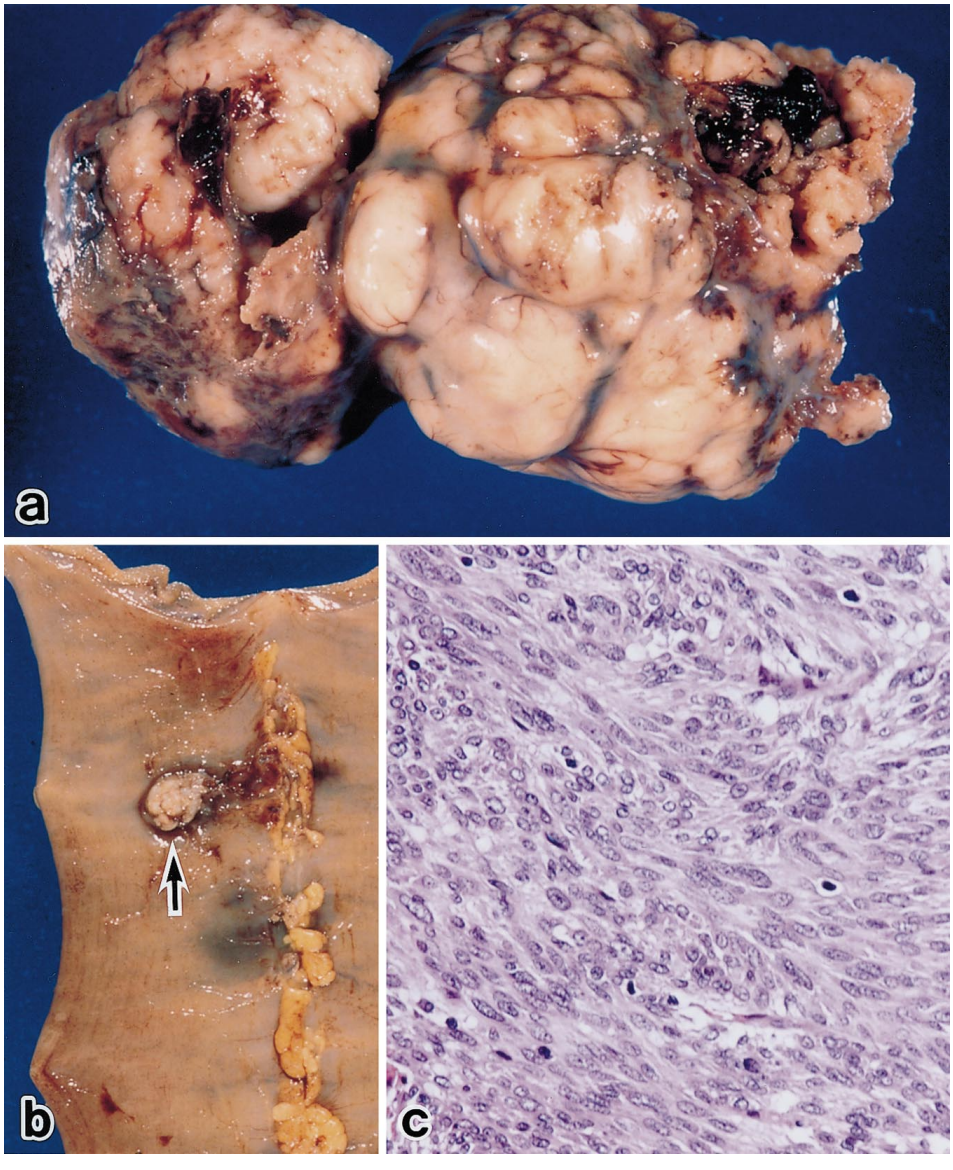

Fig. 1 **a, b** Gross and **c–e** histological findings. **a** Partially encapsulated subserosal tumour with focal haemorrhage. **b** The tumour is attached to the serosal surface of the small intestine (*arrow*). **c** The tumour consists mainly of spindle cells with a fascicular arrangement. Anisonucleosis and mitosis are prominent. HE, ×236 **d** The transitional zone between the tumour cells and nontumor nerves in Auerbach's plexus. Positive immunoreaction for S-100 protein is observed in the nontumor nerves. Streptavidin–biotin method, ×236 **e** The tumour cells show positive immunoreactions for vimentin. Streptavidin–biotin method, ×236 **f** A zonal or geographical immunostaining pattern of NSE is seen. Streptavidin–biotin method, ×117

Materials and methods

A portion of the tumour was used for conventional electron microscopy and QF-DE. For light microscopic examination, the rest of the tumour tissue was fixed in 10% buffered formalin, processed according to standard methods and embedded in paraffin. For the QF-DE method, small fragments of the tumour were fixed with 2% paraformaldehyde in 0.1 M phosphate buffer (PB), pH 7.2, for 20–30 min. They were further cut into several pieces (5×3×2 mm in size) with sharp razor blades. To remove soluble substances from the tissue surface, they were washed in PB for 30 min as previously described [12, 13]. They were postfixed with 0.25% glutaraldehyde in PB for 30 min and rinsed in 10% methanol to minimize ice crystal formation during a subsequent quick-freezing step. The prepared tissues were placed on a copper metal holder with the cut surface facing up and blotted with filter paper to remove their excess fluid. They were then quickly frozen by the metal contact method using a quick-freezing JFD-RFA machine (JEOL, Tokyo, Japan) in which the copper metal was cooled by liquid nitrogen (–196°C). They were freeze-fractured with a scalpel in the liquid nitrogen to expose well-preserved tissue areas, as previously reported [29, 30], and transferred into an EIKO FD-3AS etching machine (Eiko Company, Ibaragi, Japan). They were deeply etched under vacuum conditions ($1\sim4\times10^{-7}$ Torr) at –95°C for 10–20 min and rotary-shadowed with platinum at an angle of 30° and carbon at an angle of 90°. One drop of 2% collodion in amyl acetate was placed onto replicas as soon as the specimens were taken out from the machine, to inhibit breaking of replicas into pieces during the subsequent digestion procedure. The replicas were coated with dried collodion and were then floated on household bleach for 15–30 min to dissolve tissue components. The replica membranes were washed in distilled water and cut into small pieces with a pair of scissors. They were mounted on Formvar-filmed copper grids and immersed in amyl acetate solution to dissolve the dried collodion. All the replicas were observed in an electron microscope (Hitachi H-600) and photographed at various magnifications. For conventional electron microscopy, other tumour tissues were cut into small pieces and prefixed with 2.5% glutaraldehyde in PB at 4°C for 2 h. They were postfixed with 1% osmium tetroxide in PB at 4°C for 2 h and routinely embedded in Epon 812. Ultrathin sections were stained with uranyl acetate and lead citrate and were examined in the same electron microscope.

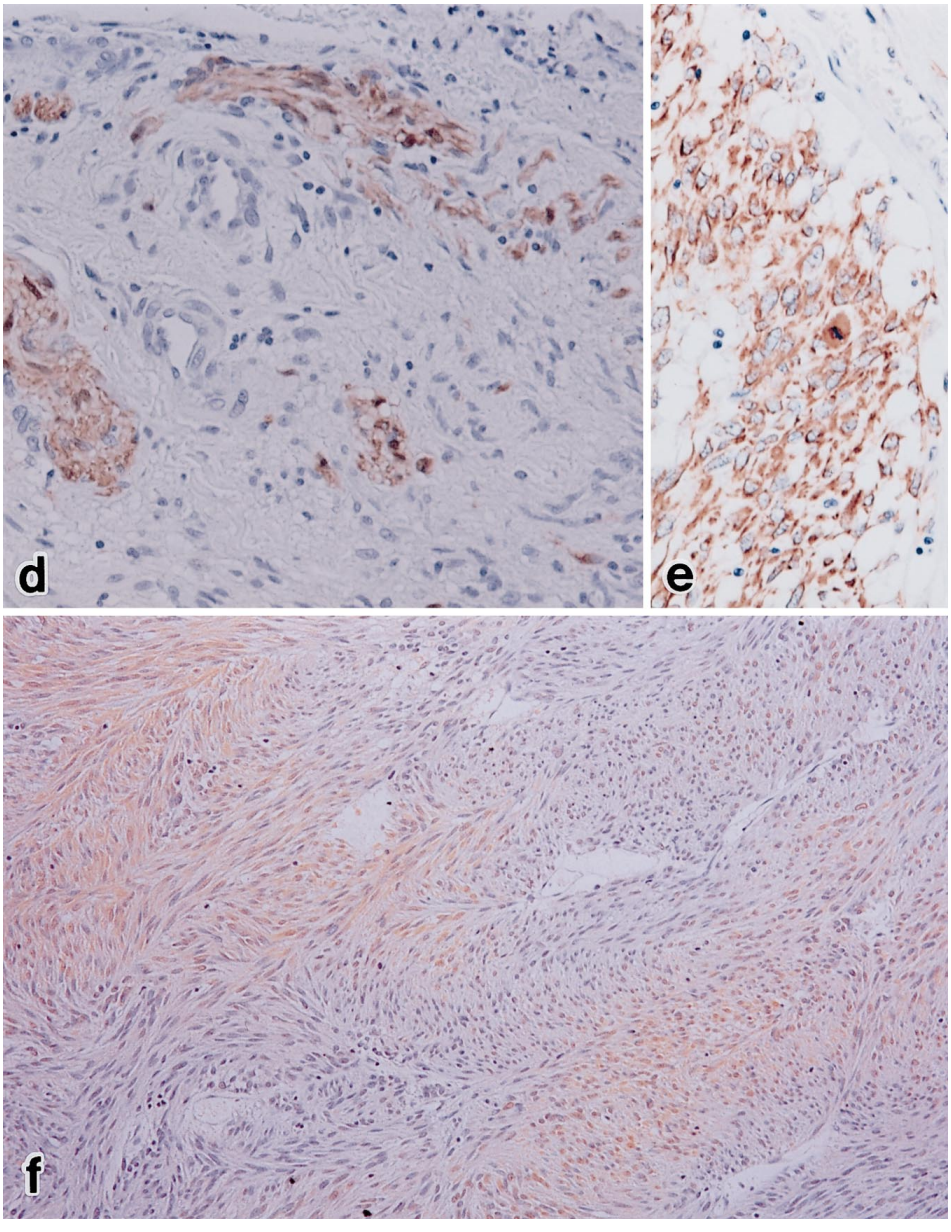

Fig. 1d–f (Legend see opposite page)

For immunohistochemistry for various antigens, the immunostaining procedure used was a streptavidin–biotin method using LSAB kit (Dako Japan, Kyoto, Japan). All antibodies used in this study are listed in Table 1. The specimen for type IV collagen immunostaining alone was pretreated with 0.4% pepsin (Sigma, St.Louis, Mo.) in 0.01 N HCl for 2 h at room temperature before addition of the primary antibody [13]. Normal mouse or rabbit serum was used as a control, replacing the individual primary antibodies.

Results

Gross examination disclosed a partially encapsulated subserosal tumour 11.5×8×7 cm in size, soft in consistency (Fig. 1a), attached to the intestinal wall of the jejunum by a narrow stalk (Fig. 1b) and extensively invading the mesentery and retroperitoneum. A small brownish area was due to mucosal haemorrhage on the tumour. The cut tissue surface showed a whitish-grey tumour with lobulation, and it also contained small spotty areas of haemorrhage and necrosis.

Histologically, some tissue areas had an epitheloid appearance, but most of the tumour cells were spindle-shaped cells with moderately hyperchromatic, elongated, and blunt-edged nuclei, and also moderate amounts of eosinophilic cytoplasm with indistinct cell borders (Fig. 1c). Some tumour cells were arranged in fascicles or whorl patterns. Anisonucleosis and mitosis were evident in other tumour cells. The stromal vascularization was prominent, and oedematous foci were observed. Muscular involvement of the tumour cells was observed in an area attached to the intestinal wall, where a transition between Auerbach nerve plexus and tumour cells was recognized (Fig. 1d), suggesting their origin from the myenteric nerve plexus.

The immunohistochemical data are summarized in Table 1. Most tumour cells showed strongly positive immunoreactions for vimentin (Fig. 1e), and also weak immunoreactions for neuron-specific enolase (NSE) and CD34 [26]. The NSE was zonally or geographically stained in the tumour and was accentuated perivascularly (Fig. 1f). In contrast, no immunoreaction for desmin, HHF35 [39], alpha smooth muscle actin (α SMA), S-100 protein, synaptophysin, chromogranin, or neurofilament was recognized in the tumour cells. The HAM-56 and α-1-antitrypsin antibodies, which are usually hallmarks for fibrohistiogenic differentiation [2, 4], showed negative immunoreactions in the present study. Both type IV collagen and laminin antibodies also showed negative immunoreactions, except for vessel walls in the tumour.

Electron microscopically, the tumour consisted of tightly packed, ovoid or elongated cells with abundant cytoplasm, containing rough-surfaced endoplasmic reticulum, mitochondria and ribosomes. Their nuclei appeared to be round to ovoid with peripheral chromatin margination (Fig. 2a). The intercellular spaces contained nodular fibrillar aggregates, which formed tangles (Fig. 2a, inset). Individual fibrils in these structures had variable widths measuring from 37 to 48 nm, and some fibrils revealed cross-banding patterns with 40- to 53-nm periodicity. They were apparently consistent with the SFs described by Min [27, 28]. In addition, many interdigitating cytoplasmic processes were often seen to form cell junctions (Fig. 2b). They also contained some cored vesicles and clear vesicles (Fig. 2c, and 2d), and bulbous synapse-like structures were present around them (Fig. 2d). Microtubules and intermediate filaments were often observed in both cytoplasm and cytoplasmic processes (Fig. 2d). No basal laminae, dense bodies, or pinocytotic vesicles were recognized.

Irregularly and loosely arranged bundles of reticular fibres were usually seen in the intercellular space (Fig. 3a). Moreover, irregular meshwork structures were seen to consist of thin filaments (7–15 nm in thickness) branching from the reticular fibres, which were clearly demonstrated on the replica membrane (Fig. 3b). They showed varying amounts of fine granular deposits along the filaments, which were mainly observed in the meshwork regions between the reticular fibres (Fig. 3b). These granules showed a tendency to produce focal lesions (Fig. 3b) and were arranged continuously on the filaments (Fig. 3c). Fully developed areas of granular deposit revealed nodular aggregated structures consisting of irregularly surfaced thick fibrils (30–48 nm in thickness) (Fig. 3d), which were compatible with the SFs observed by conventional electron microscopy. In the intervening space between the irregularly surfaced thick fibrils, many interconnecting thin filaments were detected, making up meshwork structures without granular deposits (Fig. 3e). The interconnecting filaments formed focal thickening at the connecting points along the irregularly surfaced thick fibrils, in contrast to the nonattaching regions of similar fibrils (Fig. 3e). These thick parts were arranged at periodic intervals (33–45 nm) along the fibrils, giving the periodicity of SFs that was observed by conventional electron microscopy.

Discussion

In the past decade, electron microscopic examination of some GISTs [32, 37, 41, 42] led us to accept a new category of neurogenic gastrointestinal tumour, which had both peculiar biological behaviour and a different clinical prognosis from that of nerve-sheath tumours (schwannoma and neurofibroma with or without malignancy) and neural cell tumours (ganglioneuroma and paraganglioma) of the intestinal tract [7]. A first case was reported under the diagnostic name of plexosarcoma (malignant enteric plexus tumour) by Herrera et al. in 1984 [14]. In 1986, Walker et al. [43] reported three additional cases. They used the other term “gastrointestinal autonomic nerve tumour” (GANT), to stress the origin from neural cells in the autonomic myenteric plexus.

In the present case, the tumour tissue consisted of spindle cells and showed the intensely positive immunostaining for vimentin and weak immunostaining for NSE

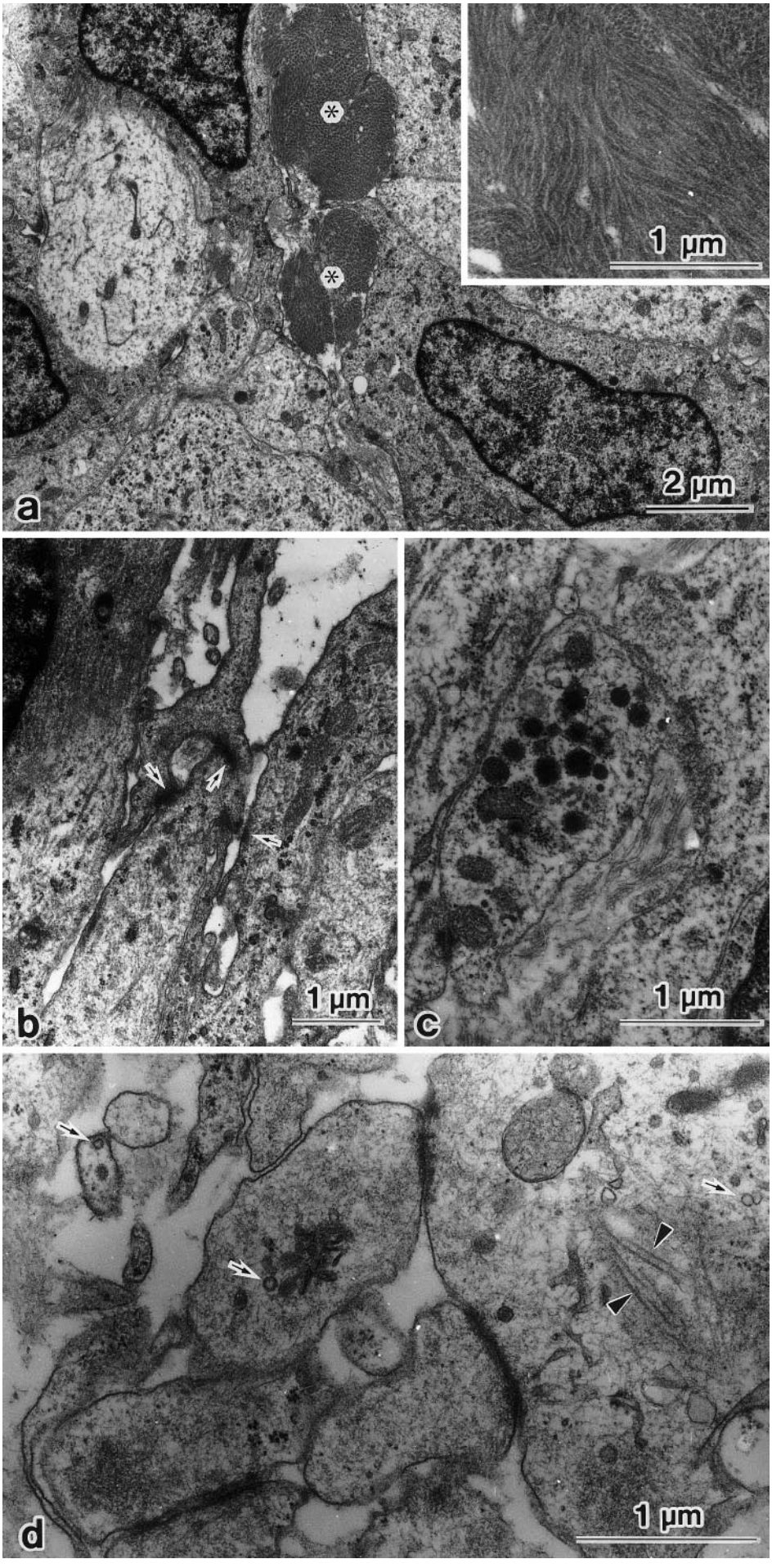

Fig. 2a–d Electron micrographs of tumour cells with skeinoid fibres (SFs). **a** Tightly packed tumour cells contained abundant cytoplasm and cell organelles. SFs are observed in the intercellular space (*asterisks*). *Inset* high-magnification view of SFs. **b** Long and interdigitating cell processes are joined together with rudimentary cell junctions (*arrows*). **c** Some cell processes contain several dense-core granules. **d** Bulbous synapse-like structures contain a few clear vesicles (*arrows*) and microtubules (*arrowheads*)

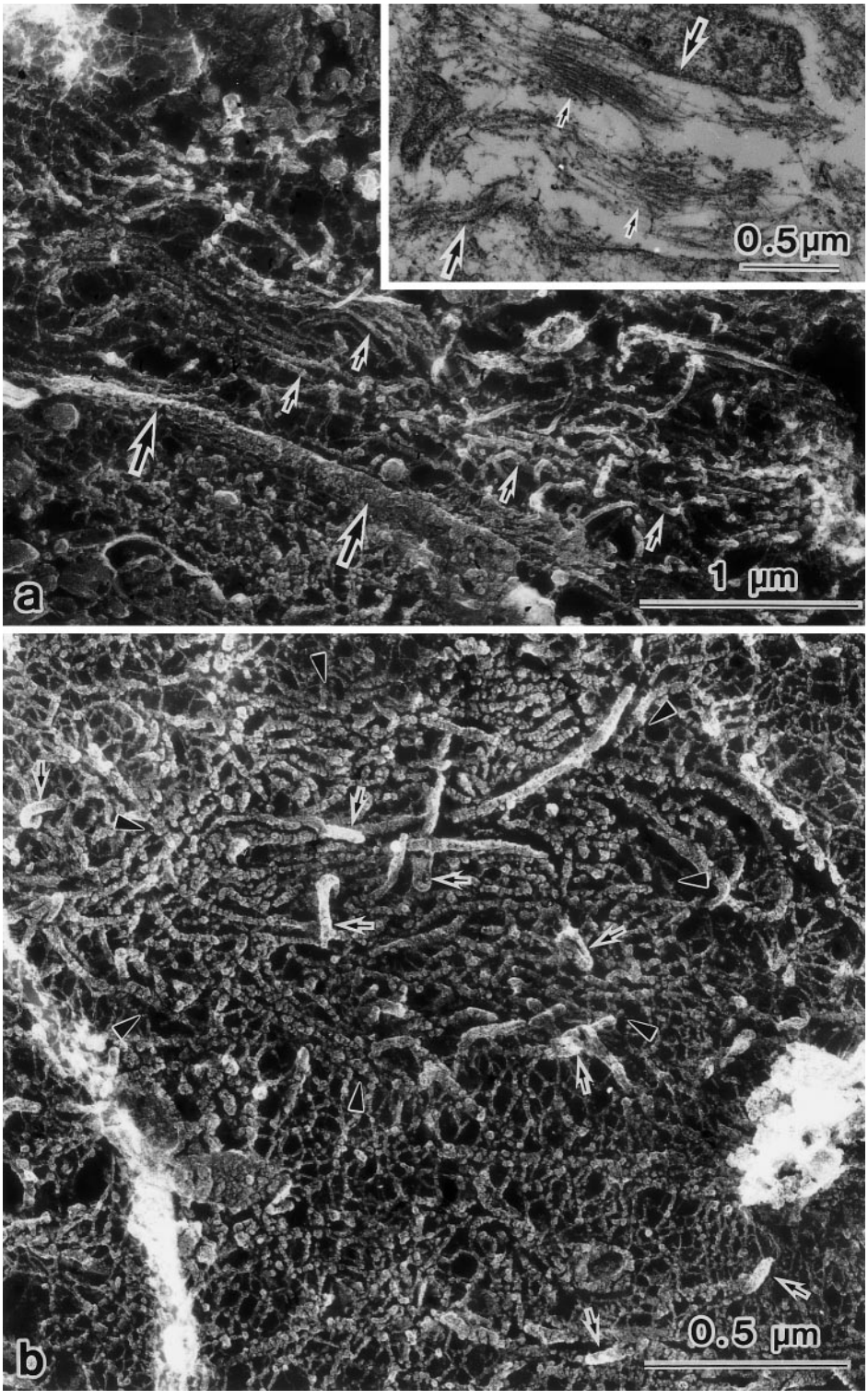

Fig. 3a–e Replica electron micrographs of tumour tissues with SFs. **a** The intercellular space contains irregularly arranged bundles of reticular fibres (*large arrows* cell membrane, *small arrows* reticular fibres. *Inset* the corresponding area in an ultrathin section. **b** Focal areas with granular deposits (demarcated by *arrowheads*) are seen in the meshwork structures, which are located between the reticular fibres (*arrows*). **c** The granular materials are continuously deposited on the filaments (*arrows*) in the meshwork structures and are arranged in parallel (*Left* stereo-electron micrographs of a replica membrane, *right* corresponding areas in an ultrathin section). **d** In this area, SFs are nodularly aggregated structures consisting of irregularly surfaced thick fibrils. **e** In intervening spaces between the irregularly surfaced thick fibrils, many interconnecting filaments are observed without the granular deposits. The connecting points (*arrows*) on the irregularly surfaced thick fibrils are thicker than the nonconnecting parts of the same fibrils, resulting in the formation of the periodicity of the thick fibrils (*Left* stereo-electron micrographs of a replica membrane, *right* corresponding areas in an ultrathin section)

and CD34. However, no immunopositive reactions were detected for other immunohistochemical markers, such as neural cells (synaptophysin, neurofilament, chromogranin), nerve sheaths (S-100 protein, type IV collagen, laminin), smooth muscle cells (desmin, α SMA, HHF35 [39], type IV collagen, laminin), and fibrohistiocytic tumour cells (HAM-56, α-1-antitrypsin) [2, 4]. Although the NSE and CD34 antibodies are immunoreactive in many nonneural tumours [11, 21, 36, 42]. The finding of NSE in the present case was similar to that of the characteristic staining pattern for GANT, as indicated by Fletcher [8] and Shanks et al. [35]. Electron microscopi-

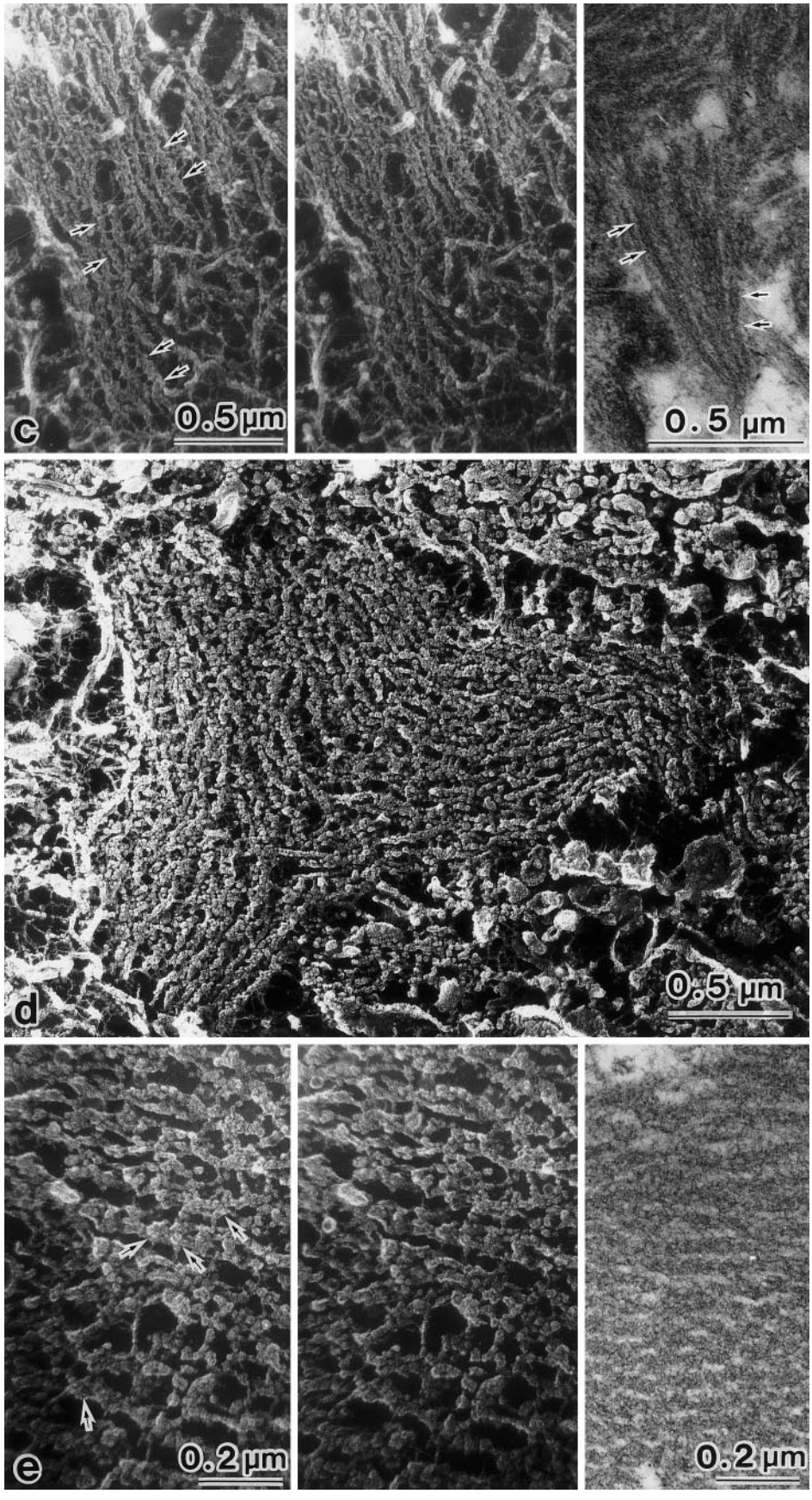

Fig. 3c–e (Legend see opposite page)

cally, the tumour cells displayed some features suggestive of neural cells in autonomic myenteric plexus, including the following characteristics: interdigitating long cell processes with occasional intercellular junctions, cytoplasmic cored vesicles, clear vesicles similar to those seen in synaptic boutons, and cytoplasmic filaments consistent with neurofilaments and neurotubules [14, 20, 43]. However, none of the electron microscopic findings commonly observed in smooth muscle tumours (basal lamina, caveolae and dense bodies) [5], schwannomas (basal lamina) [6], paragangliomas (numerous neurosecretory granules scattered throughout the cytoplasm) [18, 33, 43] and fibrohistiocytic tumours (well-developed rER, many lysosomes, erythro- and/or haemosidero-phagocytotic vacuoles, and filopodia) [40] were recorded. In the present case, when both light and electron microscopic and immunohistochemical findings were considered the tumour was finally diagnosed as GANT.

Clinically, GANTs are more common in adults, especially in men, over the age of 40, and the tumour sizes vary from 5 to 20 cm. The common sites are stomach, small intestine and retroperitoneum [3, 14, 15, 20], but a case of oesophageal GANT was recently reported [19]. The clinical symptoms vary, including an enlarging abdominal mass, abdominal pain and gastrointestinal bleeding [14, 15, 22]. In general, the tumour masses are brain-like in having a soft consistency and have a tendency to pronounced vascularity compared with other GISTs [20]. Invasive behaviour, including peritoneal involvement and hepatic metastasis, is also one of their characteristics [15, 22].

In the present case, the patient suffered from a local recurrence twice after the first resection of the primary tumour, and the tumour had a very aggressive course. Origin of the lesion from Auerbach's myenteric plexus was suggested by the light microscopic examination, but the main tumour mass involved the retroperitoneum and mesentery extensively. Although the patient was admitted to hospital because of a large amount of intestinal bleeding, neither obvious ulcers nor erosive lesions were detected. Tumours such as this one differ from other types of GIST in that the exophytic-growth from the intestinal wall and the sparse mucosal lesions are thought to be important pathologic features of GANTs.

SFs were demonstrated ultrastructurally in the present case. According to Min's report [27, 28], SFs were found only in 3 cases of neurogenic spindle cell tumour and 8 cases of small intestinal stromal tumours among more than 5000 cases studied by electron microscopy. Min stated that SF was an ultrastructural marker for neurogenic spindle cell tumours and that the 8 cases of small intestinal stromal tumours with SFs might be of neurogenic origin. After his report, SFs were found in many cases of neurogenic spindle cell tumours including GANTs [9, 16, 24], although there were exceptional cases [23, 25] and the contrasting opinion, that the SFs were not an exclusive neurogenic marker [10, 41], was also expressed. In previous reports, periodic acid–Schiff-positive patterns, but negative staining with phosphotungstic acid-haematoxylin, elastica van Gieson and reticulin silver impregnation has been described. In contrast, Masson trichrome stained them blue [28]. Immunohistochemically, neither type IV collagen nor laminin was found [28]. Ishida et al. [16] reported that SFs might not contain proteoglycans, according to negative staining results for cuprolinic blue and polyethyleneimine. Tsang [38] and Ojanguren et al. [31] argued that the SFs were related to the tumour differentiation and that well-differentiated tumours might produce more prominent SFs. In the present case, the amount of SFs was too small to be observed by light microscopy, because it was assumed to be due to the poor differentiation of the tumour cells. The findings in the present case support the opinion of Tsang [38] and Ojanguren et al. [31].

Our original finding was a three-dimensional ultrastructure for SFs, as revealed by the QF-DE method. The meshwork structures were clearly demonstrated in the intercellular space, which contained focal areas of finely granular deposits. These granules revealed a tendency to be deposited along the filaments in a linear or continuous fashion and often showed a parallel arrangement.

Granular deposition on pre-existing meshwork structures is considered to be the essential cause of SF development. We were not able to confirm the composition of the meshwork structures or the nature of the granules. Such a meshwork seems to be common in pericellular areas in various cell types. Our previous report and other' reports on studies involving the QF-DE method have indicated their existence in pericellular areas of tumour cells in leiomyosarcoma [13] and the normal cells of the pancreas, placenta and oral mucosa [1]. However, the constituents of the meshwork vary, depending on the cell types involved [1]. The characteristic linear arrangement of granular deposit is thought to be a rearrangement of the meshwork accompanied by the deposition, or the selective occurrence of deposition along certain types of filaments, which showed a linear or parallel arrangement in the meshwork. Further, we clearly observed many interconnecting thin filaments between the irregularly surfaced thick fibrils, which were pre-existing components in the meshwork, avoiding the granular deposits. The periodicity of the SFs was thought to be due to the connection between irregularly surfaced thick fibrils and interconnecting thin filaments. Whether or not SFs are an exclusive marker for neurogenic spindle cell tumours is still the subject of debate; we have concluded that a relationship between the composition of the meshwork and the granular materials produced by the tumour cells is important for SF development.

Recently Kindblom et al. [17] stated that GIST, including GANT, exhibited striking similarities with the interstitial cell of Cajal and might originate from a stem cell that has differentiated toward a pacemaker cell phenotype.

For these reasons, they proposed a diagnostic name of gastrointestinal pacemaker cell tumour to replace GIST. Their hypothesis at variance with our opinion, because of the intimate association between the Auerbach's plexus and the tumour cells observed in the present case. Clarification of the histogenesis and nature of SFs will be a key point in the resolution of the many problems with regard to origin, differentiation, nomenclature, and prediction of prognosis of GANT and the other GISTs.

References

1. Adachi E, Hayashi T (1994) Anchoring of epithelia to underlying connective tissue: Evidence of frayed ends of collagen fibrils directly merging with meshwork of lamina densa. J Electron Microsc 43:264–271
2. Adams CW, Poston RN (1990) Macrophage histology in paraffin-embedded multiple sclerosis plaques is demonstrated by the monoclonal pan-macrophage marker HAM-56: Correlation with chronicity of the lesion. Acta Neuropathol 80:208–211
3. Dhimes P, López-Carreira M, Ortega-Serrano MP, García-Muñoz H, Martínez-Gonzales MA, Ballestín C (1995) Gastrointestinal autonomic nerve tumours and their separation from other gastrointestinal stromal tumours: an ultrastructural and immunohistochemical study of seven cases. Virchows Arch 426:27–35
4. DuBoulay G (1982) Demonstration of alpha-1-antitrypsin and alpha-1-antichymotrypsin in fibrous histiocytomas using the immunoperoxidase technique. Am J Surg Pathol 6:559–564
5. Enzinger FM, Weiss SW (1988) Soft tissue tumors, 2nd edn. Mosby, St Louis, Washington DC Toronto, pp 402–421
6. Enzinger FM, Weiss SW (1988) Soft tissue tumors, 2nd edn. Mosby. St. Louis, Washington DC, Toronto, pp 781–815
7. Fenoglio-Preiser CM, Pascal RR, Perzin KH (1988) Tumors of the intestine. In: Atlas of tumor pathology. Armed Forces Institute of Pathology, Washington, DC, pp 454–473
8. Fletcher CDM (1995) Diagnostic histopathology of tumors, vol 2. Churchill Livingstone. New York, pp 111–121
9. García-Rostán y Pérez GM, Díaz MM, Bragado FG (1997) Jejunal stromal tumor with skeinoid fibers of myenteric plexoma: A case report. Pathol Int 47:794–800
10. Goldblum JR, Appelman HD (1995) Stromal tumors of the duodenum. A histologic and immunohistochemical study of 20 cases. Am J Surg Pathol 19:71–80
11. Haimoto H, Takahashi Y, Koshikawa T, Nagura H, Kato K (1985) Immunohistochemical localization of γ-enolase in normal human tissues other than nervous and neuroendocrine tissues. Lab Invest 52:257–263
12. Hemmi A, Komiyama A, Ohno S, Fujii Y, Kawaoi A, Katoh R, Suzuki K (1995) Different organization of intermediate filaments in columnar cells of rat large intestinal mucosa as revealed by confocal laser scanning microscopy and quick-freezing and deep-etching method. Virchows Arch 426:401–410
13. Hemmi A, Komiyama A, Ohno S, Fujii Y, Katoh R, Yokoyama A, Kawaoi A (1998) Poorly differentiated desmin-negative and vimentin-positive leiomyosarcoma of the stomach examined by the immunohistochemical and quick-freezing and deep-etching methods. Virchows Arch 432: 377–383
14. Herrera GA, De Moraes HP, Grizzle WE, Han SG (1984) Malignant small bowel neoplasm of enteric plexus derivation (plexosarcoma): light and electron microscopic study confirming the origin of the neoplasm. Dig Dis Sci 29:275–284
15. Herrera GA, Cerezo L, Jones JE, Sack J, Grizzle WE, Pollack WJ, Lott RL (1989) Gastrointestinal autonomic nerve tumors. 'Plexosarcomas'. Arch Pathol Lab Med 113:846–853
16. Ishida T, Wada I, Horiuchi H, Oka T, Machinami R (1996) Multiple small intestinal stromal tumors with skeinoid fibers in association with neurofibromatosis 1 (von Recklinghausen's disease). Pathol Int 46:689–695
17. Kindblom LG, Remotti HE, Aldenborg F, Meis-Kindblom LM (1998) Gastrointestinal pacemaker cell tumor (GIPACT): gastrointestinal stromal tumors show phenotypic characteristics of the interstitial cells of Cajal. Am J Pathol 152:1259–1269
28. Konok GP, Sanchez-Cassis G (1979) Gangliocytic paraganglioma of the duodenum. Can J Surg 22:173–175
19. Lam KY, Law SYK, Chu KM, Ma LT (1996) Gastrointestinal antonomic nerve tumor of the esophagus: A clinicopathologic, immunohistochemical study of a case and review of the literature. Cancer 78:1651–1659
20. Lauwers GY, Erlandson RA, Casper ES, Brennan MF, Woodruff JM (1993) Gastrointestinal autonomic nerve tumors: a clinicopathological, immunohistochemical, and ultrastructural study of 12 cases. Am J Surg Pathol 17:887–897
21. Leader M, Collins M, Patel J, Henry K (1986) Antineuron specific enolase staining reactions in sarcomas and carcinomas. Its lack of neuroendocrine specificity. J Clin Pathol 39:1186–1192
22. MacLeod CB, Tsokos M (1991) Gastrointestinal autonomic nerve tumor. Ultrastruct Pathol 15:49–55
23. Matsukuma S, Doi M, Suzuki M, Ikegawa K, Sato K, Kuwabara N (1997) Numerous eosinophilic globules (skeinoid fibers) in a duodenal stromal tumor: An exceptional case showing smooth muscle differentiation. Pathol Int 47:789–793
24. Matsumoto K, Min W, Yamada N, Asano G (1997) Gastrointestinal autonomic nerve tumors: Immunohistochemical and ultrastructural studies in cases of gastrointestinal stromal tumor. Pathol Int 47:308–314
25. Mentzel T, Katenkamp D (1996) Gastrointestinal stromal tumour with skeinoid fibers and bidirectional immunohistochemical differentiation. Histopathology 29:175–177
26. Miettinen M, Virolainen M, Maarit-Sarlomo-Rikala (1995) Gastrointestinal stromal tumors – value of CD 34 antigen in their identification and separation from true leiomyomas and schwannomas. Am J Surg Pathol 19:207–216
27. Min KW (1991) Skeinoid fibers: an ultrastructural marker of neurogenic spindle cell tumors. Ultrastruct Pathol 15:603–611
28. Min KW (1992) Small intestinal stromal tumors with skeinoid fibers: Clinicopathological, immunohistochemical, and ultrastructural investigations. Am J Surg Pathol 16:145–155
29. Naramoto A, Ohno S, Furuta K, Itoh N, Nakazawa K, Nakano M, Shigematsu H (1991) Ultrastructural studies of hepatocyte cytoskeletons of phalloidin-treated rats by quick-freezing and deep-etching method. Hepatology 13:222–229
30. Ohno S, Fujii Y (1991) Three-dimensional studies of the cytoskeleton of cultured hepatocytes: a quick-freezing and deep-etching study. Virchows Arch [A] 418:61–70
31. Ojanguren I, Ariza A, Navas-Palacios JJ (1996) Gastrointestinal autonomic nerve tumor: Futher observations regarding an ultrastructural and immunohistochemical analysis of six cases. Hum Pathol 27: 1311–1318
32. Rosai J (1996) Gastrointestinal tract. In: Ackerman's surgical pathology, 8th edn, vol 1. Mosby, St Louis, pp 645–647
33. Scheithauer BW, Nora FE, LeChago J, Wick MR, Crawford BG, Weiland LH, Carney JA (1986) Duodenal gangliocytic paraganglioma. Clinicopathologic and immunocytochemical study of 11 cases. Am J Clin Pathol 86:559–565
34. Segal A, Carello S, Caterina P, Papadimitriou JM, Spagnolo DV (1994) Gastrointestinal autonomic nerve tumors: a clinicopathological, immunohistochemical and ultrastructural study of 10 case. Pathology 26:439–447
35. Shanks JH, Harris M, Banerjee SS, Eyden BP (1996) Gastrointestinal autonomic nerve tumorurs: a report of nine cases. Histopathology 29:111–121
36. Sirgi KE, Wick MR, Swanson PE (1993) B72.3 and CD34 immunoreactivity in malignant epithelioid soft tissue tumors: ad-

junctions in the recognition of endothelial neoplasms. Am J Surg Pathol 17:179–185
37. Tirabosco R, Cavazzana AO, Santeusanio G, Spagnoli LG (1995) Gastrointestinal stromal tumor: evidence for a smooth-muscle origin. Mod Pathol 8:193–196
38. Tsang WYW (1994) Gastrointestinal autonomic nerve (GAN) tumors: an underrecognized group of gastrointestinal stromal neoplasm. Adv Anat Pathol 1:21–28
39. Tsukada T, McNutt MA, Ross R, Gown AM (1987) HHF35, a muscle actin-specific monoclonal antibody. II. Reactivity in normal, reactive, and neoplastic human tissues. Am J Pathol 127:389–402
40. Tsuneyoshi M, Enjoji M, Shinohara N (1981) Malignant fibrous histiocytoma: an electron microscopic study of 17 cases. Virchows Arch [A] 392:135–145
41. Tworek JA, Appelman HD, Singleton TP, Greenson JK (1997) Stromal tumors of the jejunum and ileum. Mod Pathol 10:200–209
42. Van de Rijn M, Hendrickson MR, Rouse RV (1994) CD34 expression by gastrointestinal tract stromal tumors. Hum Pathol 25:766–771
43. Walker P, Dvorak A (1986) Gastrointestinal autonomic nerve (GAN) tumor: ultrastructural evidence for a newly recognized entity. Arch Pathol Lab Med 110:309–316